Time dependent *CP* violation measurements at Belle II

C. Antonioli([1])([2])([*]) on behalf of the Belle II italian collaboration

([1]) *Dipartimento di Fisica e Astronomia, Università degli Studi di Padova - Padova, Italy*
([2]) *INFN, Sezione di Padova - Padova, Italy*

Summary. — Time dependent *CP* violation phenomena allow to precisely measure fundamental parameters of the Standard Model and search for New Physics. The Belle II experiment successfully completed the first phase of data tacking, collecting a sample of e^+e^- annihilations corresponding to an integrated luminosity of 362 fb^{-1} at the $\Upsilon(4S)$ resonance. In this report we present the latest measurement of time dependent *CP* violation in the golden channel $B^0 \to J/\psi K^0_S$. This study uses for the first time a new flavour tagging algorithm, based on graph-neural-network, which increases the effective tagging efficiency by 18% (relative) compared to the previous algorithm. Finally, we present the first Belle II measurement in the channel $B^0 \to \eta' K^0_S$, which is dominated by the loop amplitude.

1. – Introduction

In the Standard Model (SM), the non-invariance of the weak interactions with respect to the combined application of charge conjugation (C) and parity (P) transformations is explained by the Cabibbo-Kobayashi-Maskawa (CKM) mechanism [1]. The *CP* violation (*CPV*) arises from an irreducible complex phase in the so-called CKM matrix, a 3×3 unitary complex matrix that rotates the mass eigenstates into the flavour eigenstates. The unitarity condition of the CKM matrix implies $V_{ud}V^*_{ub} + V_{cd}V^*_{cb} + V_{td}V^*_{tb} = 0$ which can be represented by a triangle in the complex plane known as Unitary Trangle (UT). By measuring in an independent way all sides and angles of the UT, we can check experimentally if the triangle "closes". If this were not the case, then it would be the evidence of New Physics (NP).

The measurements of the mixing-induced *CPV* in B^0 meson decays, *i.e.* *CPV* resulting from the oscillation between B^0 and $\overline{B}^0$, provide constraints on the values of the UT angles ϕ_1 and ϕ_2([1]). In fig. 1 we show the current global fit results for the UT parameters.

([*]) E-mail: cecilia.antonioli@pd.infn.it
([1]) These angles are also known as β and α.

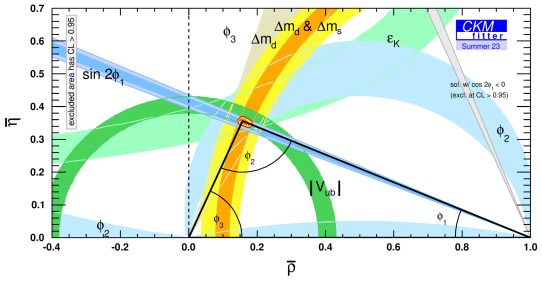

Fig. 1. – Current constraints on the UT [2].

The angle ϕ_1 can be measured with high precision in the tree-dominated $b \to c\bar{c}s$ decays, *e.g.* $B^0 \to J/\psi K^0_S$, and in the loop-dominated $b \to s\bar{q}q$ decays ($q = u, d, s$), such as $B^0 \to \eta' K^0_S$. A comparison between *CP* asymmetries measured precisely in $b \to c\bar{c}s$ and $b \to s\bar{q}q$ transitions can probe NP effects in the loops.

2. – Belle II

Belle II [3] is a particle physics experiment operating at the SuperKEKB [4] energy-asymmetric e^+e^- collider in Tsukuba, Japan. The vast majority of data are taken at the centre-of-mass energy $\sqrt{s} = 10.58$ GeV corresponding to the $\Upsilon(4S)$ resonance, the lightest that can decay strongly to a pair of B mesons. The asymmetric beam energies provide a Lorentz boost to the centre-of-mass system with $\beta\gamma = 0.28$, allowing time dependent *CPV* measurements. The detector has a cylindrical structure around the beam pipe, while it has a significant forward-backward asymmetry to improve the solid angle acceptance in the boost (forward) direction. The innermost part of the detector comprises a two-layer silicon pixel detector (PXD), surrounded by a four-layer double-sided silicon microstrip detector (SVD). Together, they provide information about the charged particle trajectories (tracks) and B decay positions (vertices). The momentum and charge of charged particles are reconstructed with a 56-layer central drift chamber (CDC), which is the main tracking subsystem. Charged particle identification (PID) is performed by a time-of-propagation (TOP) counter and an aerogel ring-imaging Cherenkov (ARICH) counter, located in the barrel and forward-endcap regions, respectively. The CDC provides additional PID information through the measurement of specific ionisation. An electromagnetic calorimeter (ECL), made of CsI(Tl) crystals, is used to measure the energies and times of detection of photons and electrons. The tracking, PID, and ECL subsystems are surrounded by a superconducting solenoid, providing an axial magnetic field of 1.5 T. A K^0_L and muon identification system (KLM) is located outside of the magnet and consists of flux-return iron plates interspersed with resistive plate chambers and plastic scintillators.

3. – Time dependent *CP* asymmetry

At SuperKEKB, the $B^0\overline{B}^0$ pairs are produced via the process $e^+e^- \to \Upsilon(4S) \to B^0\overline{B}^0$. For time dependent *CPV* measurements we consider events when one neutral B meson ($B_{\rm tag}$) decays into a flavour-specific final state at time $t_{\rm tag}$, while the other B meson ($B_{\rm sig}$) decays into a *CP* eigenstate at time t_{CP}. Since the two neutral B mesons

remain in a quantum-entangled state until one of them decays, tagging the flavour of B_{tag} at the time of its decay determines the flavour of B_{sig} at the same time. We define q_{tag} as the flavour of B_{tag} at t_{tag} (+1 for B^0, −1 for $\overline{B}^0$). The decay rate for the $B_{\text{sig}} \to f_{CP}$ is given by

$$\mathcal{P}(\Delta t, q_{\text{tag}}) = \frac{e^{-|\Delta t|/\tau_{B^0}}}{4\tau_{B^0}}[1 + q_{\text{tag}}\mathcal{A}_{CP}(\Delta t)] \tag{1}$$

where $\Delta t = t_{CP} - t_{\text{tag}}$ is the proper-time difference, τ_{B^0} is the B^0 lifetime, and $\mathcal{A}_{CP}$ is the time dependent *CP* asymmetry defined as

$$\mathcal{A}_{CP}(\Delta t) = \frac{\Gamma(\overline{B}^0 \to f_{CP}) - \Gamma(B^0 \to f_{CP})}{\Gamma(\overline{B}^0 \to f_{CP}) + \Gamma(B^0 \to f_{CP})} = S\sin(\Delta m_d \Delta t) - C\cos(\Delta m_d \Delta t) \tag{2}$$

where Δm_d is the mass difference between the two neutral B meson mass eigenstates. S and C are the parameters of interest and quantify the mixing-induced and the direct *CPV*, respectively. In the SM, $S = \sin 2\phi_1$ and $C = 0$ with good precision.

Experimentally, the *CP* asymmetries can be extracted from a fit to the $\mathcal{P}(\Delta t, q_{\text{tag}})$ distribution. A crucial experimental aspect in the measurement of S and C is the determination of the initial flavour of the B mesons. At B factories, the B mesons are boosted and have significant momentum in the laboratory frame. Consequently, Δt is determined from the relative displacement of the B decay vertices Δz.

In the following we will present the new flavour tagging algorithm, based on graph-neural-network. Afterwards, we will present the time dependent *CPV* measurements using Belle II data collected between 2019 and 2022 (Run I), corresponding to an integrated luminosity of 362 fb^{-1} at the $\Upsilon(4S)$ resonance.

4. – New flavour tagger GFlaT

GFlaT [5] is a new algorithm that uses a graph-neural-network to determine the flavour of neutral B mesons. The algorithm is designed to run after B_{sig} is reconstructed and uses information from the tracks and cluster energy deposits that are not associated with B_{sig}. We refer to these tracks and clusters as the rest of the event (ROE).

Flavour tagging is possible because many decay modes of neutral B mesons provide flavour signatures through flavour-specific final states. The old flavour tagging algorithm, known as the category-based flavour tagger [6], identifies B^0 decay products and then combines all information to determine the B^0 flavour. The algorithm provides as output the product qr, where q is the flavour of the B_{tag} meson, and r the dilution factor. By definition, the dilution factor r is equal to $1 - 2w$, where w corresponds to the fraction of wrongly tagged events. A dilution factor of $r = 0$ indicates that is not possible to distinguish between B^0 and $\overline{B}^0$, whereas a dilution factor of $r = 1$ indicates a perfectly tagged flavour.

GFlaT improves flavour tagging by accounting for the information in the category-based flavour tagger as well as the correlations between information from final state particles. In the context of graph-neural-networks, the set of ROE charged particles is a graph with each particle a node and each pair an edge. The algorithm processes as input variables for each ROE charged particle the momentum, tracking and PID information, as well as the products of the charge of the particle and the output of the category-based flavour tagger for each category.

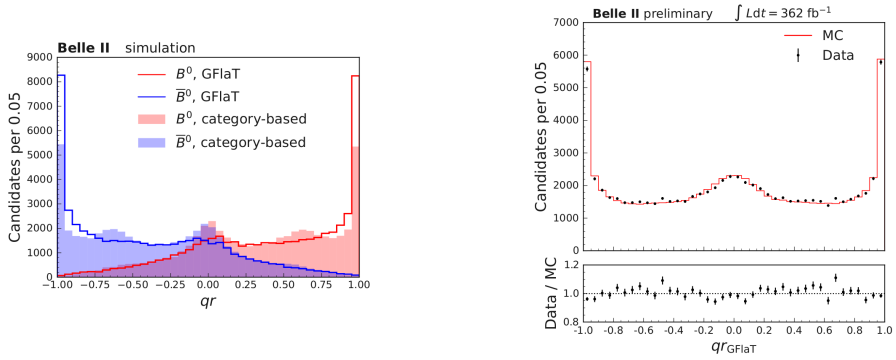

Fig. 2. – Distributions of qr for true B^0 and $\overline{B}^0$ from GFlaT and the category-based flavour tagger in simulated data (left). Distributions of qr_{GFlaT} for $B^0 \to D^{(*)-}\pi^+$ in background-subtracted data and correctly reconstructed simulated events normalised to the data signal yield (right).

GFlaT was trained on Monte Carlo simulated B decays. Figure 2 (left) shows the qr distributions for true B^0 and $\overline{B}^0$ for independent test data consisting of 10^5 events from GFlaT and the category-based flavour tagger. It is evident that GFlaT better distinguishes between B^0 and $\overline{B}^0$ than the category-based flavour tagger. The peaks at $|qr| \approx 1$ are higher and the bumps at $|qr| \approx 0$ and $|qr| \approx 0.65$ are smaller.

The performance of GFlaT was also evaluated by using events $B_{\mathrm{sig}} \to D^{(*)-}\pi^+$. The analysed data set correspond to 362 fb^{-1} collected with the Belle II detector in Run I. The flavour of B_{sig} is determined by the charge of the pion. Figure 2 (right) shows the qr_{GFlaT} distribution in background-subtracted data and correctly reconstructed simulated events normalised to the data signal yield.

GFlaT achieves an effective tagging efficiency of $\varepsilon_{\mathrm{tag}} = (37.40 \pm 0.43 \pm 0.36)\%$, where the first uncertainty is statistical and the second systematic. We obtain a 18% relative increase in the effective tagging efficiency compared to the previous Belle II algorithm (the category-based effective tagging efficiency is $\varepsilon_{\mathrm{tag}} = (31.68 \pm 0.45(\mathrm{stat.}))\%$).

5. – Time dependent CPV in $B^0 \to J/\psi K^0_S$

The $B^0 \to J/\psi K^0_S$ decay proceeds through $b \to c\bar{c}s$ transitions. Subleading corrections from penguin amplitudes are expected to be very small, making this decay the "golden mode" for the determination of $\sin 2\phi_1$. Belle II utilises the full Run I data set to measure the CP asymmetries S and C in the $B^0 \to J/\psi K^0_S$ decays [5]. We reconstruct J/ψ candidates via $J/\psi \to e^+e^-$ or $\mu^+\mu^-$, the neutral kaon candidates via $K^0_S \to \pi^+\pi^-$. The B_{tag} flavour is determined with the GFlaT tagging algorithm. We perform extended unbinned likelihood fits to the energy difference distributions $\Delta E = E^* - E_{\mathrm{beam}}$ (E^* is the B^0 energy and $E_{\mathrm{beam}} = \sqrt{s}/2$ is the beam energy, both in the centre-of-mass frame) in order to determine the signal and background yields and shapes. We show the ΔE distribution and the fit result in fig. 3 (left). The CPV parameters S and C are determined by performing a simultaneous fit to the background-subtracted Δt distributions. Figure 3 (right) shows the background-subtracted Δt distributions for B^0 and $\overline{B}^0$ tagged events and the result of the fits. The results are: $S = (0.724 \pm 0.035 \pm 0.014)$ and $C = (-0.035 \pm 0.026 \pm 0.013)$, where the first uncertainty is statistical and the second

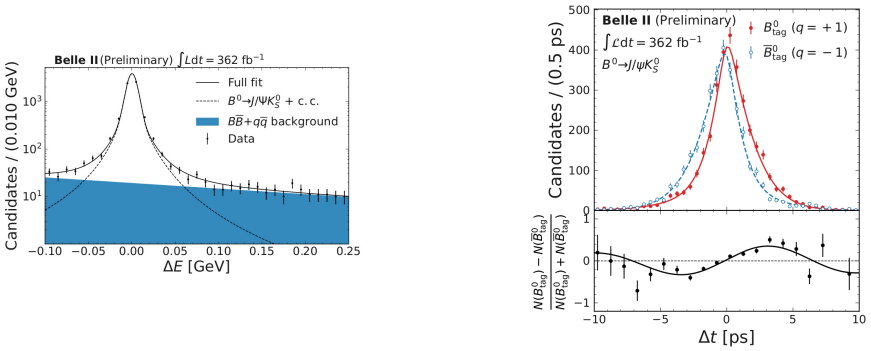

Fig. 3. – Distributions of ΔE for $B^0 \to J/\psi K^0_S$ and the best-fit function (left). Background-subtracted Δt distribution for $B^0 \to J/\psi K^0_S$ and the best-fit function, separately for B^0 and $\overline{B}^0$ tagged events. The bottom panel shows the *CP* asymmetry (right).

systematic. These results are in agreement with the world averages $S = (0.699 \pm 0.017)$ and $C = (-0.005 \pm 0.015)$ [7]. From S, we calculate $\phi_1 = (23.2 \pm 1.5 \pm 0.6)^\circ$.

6. – Time dependent *CPV* in $B^0 \to \eta' K^0_S$

The $B^0 \to J/\psi K^0_S$ decay proceeds through $b \to s\bar{q}q$ gluonic penguin transitions. This decay is of particular interest due to its relatively large branching fraction and limited contribution from tree amplitudes. We analyse the the full Belle II Run I data set to measure the *CP* asymmetries S and C in the $B^0 \to \eta' K^0_S$ decays [8]. The signal events are obtained through the reconstruction of neutral kaon candidates via $K^0_S \to \pi^+\pi^-$ and the reconstruction of η' meson candidates via two channels, $\eta' \to \eta(\to \gamma\gamma)\pi^+\pi^-$ and $\eta' \to \rho(\to \pi^+\pi^-)\gamma$. The $B_{\rm tag}$ flavour is determined with the category-based tagging algorithm. The parameters S and C are extracted with an extended unbinned maximum-likelihood fit to the distributions of Δt and other observables that discriminate signal from background. These observables are the energy difference ΔE, the beam-energy constrained mass $M_{\rm bc} = \sqrt{s/4 - p^{*2}}$, where p^* is the B^0 momentum in the centre-of-

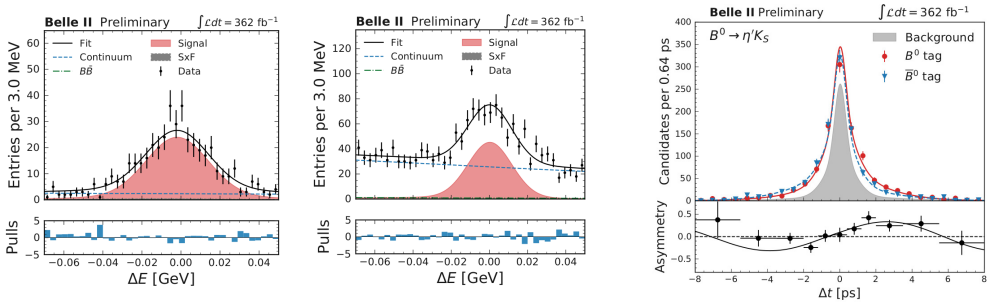

Fig. 4. – Distribution of ΔE for $B^0 \to \eta'[\to \eta(\to \gamma\gamma)\pi^+\pi^-]K^0_S$ and $B^0 \to \eta'[\to \rho(\to \pi^+\pi^-)\gamma]K^0_S$, and the best-fit functions (left). Distribution of Δt for $B^0 \to \eta' K^0_S$ and the best-fit function, separately for B^0 and $\overline{B}^0$ tagged events. The background contribution is shown as a shaded area. The bottom panel shows the *CP* asymmetry (right).

mass frame, and the boosted-decision-tree (BDT) output $C_{\rm BDT}$ used to separate $B\overline{B}$ and continuum events based on their topologies. As example, we show the distribution of the fit observable ΔE for the two subchannels in fig. 4 (left). The Δt distributions are shown separately for B^0 and $\overline{B}^0$ tagged events in fig. 4 (right) by combining the two subchannels. The results for *CPV* parameters from a simultaneous fit of the two subchannels are: $S = (0.67 \pm 0.10 \pm 0.04)$ and $C = (-0.19 \pm 0.08 \pm 0.03)$, where the first uncertainty is statistical and the second systematic. This is the first measurement of *CPV* in this channel at Belle II. The results are in agreement with the current world averages $S = (0.63 \pm 0.06)$ and $C = (-0.05 \pm 0.04)$ [7].

7. – Conclusions

We have presented the most recent measurements of time dependent *CPV* performed by the Belle II experiment using Run I data. The *CP* asymmetries S and C measured for $B^0 \to J/\psi K^0_S$ and $B^0 \to \eta' K^0_S$ are in good agreement with the world averages and within the SM predictions.

The GFlaT algorithm has an 18% better effective tagging efficiency compared to the category-based flavour tagger, which is equivalent to having 18% more luminosity.

In February 2024, data collection for Run II resumed. Therefore, new data sets for time dependent *CPV* measurements will be available in the future.

REFERENCES

[1] Kobayashi M. and Maskawa T., *Prog. Theor. Phys.*, **49** (1973) 652.
[2] Charles J. *et al.*, *Eur. Phys. J. C*, **41** (2005) 1-131, updated results and plots available at `http://ckmfitter.in2p3.fr`.
[3] Kou E. *et al.*, *PTEP*, **2019** (2019) 123C01 [Erratum: *PTEP*, **2020** (2020) 029201].
[4] Akai K., Furukawa K. and Koiso H., *Nucl. Instrum. Meth. A*, **907** (2018) 188.
[5] Adach I. *et al.*, *A new graph-neural-network flavor tagger for Belle II and measurement of* $\sin 2\phi_1$ *in* $B^0 \to J/\psi K^0_S$ *decays*, arXiv:2402.17260 (2024).
[6] Abudinén F. *et al.*, *Eur. Phys. J. C*, **82** (2022) 283.
[7] Amhis Y. *et al.*, *Phys. Rev. D*, **107** (2023) 052008, updated results and plots available at `https://hflav.web.cern.ch/`.
[8] Adach I. *et al.*, *Measurement of CP asymmetries in* $B^0 \to \eta' K^0_S$ *decays at Belle II*, arXiv:2402.03713 (2024).